

Geometrical Penrose Tilings have Finite Type

Victor Lutfalla* Thomas Fernique†

Abstract Rhombus Penrose tilings are tilings of the plane by two decorated rhombi such that the decoration match at the junction between two tiles (like in a jigsaw puzzle). In dynamical terms, they form a tiling space of finite type. If we remove the decorations, we get, by definition, a sofic tiling space that we here call geometrical Penrose tilings. Here, we show how to compute the patterns of a given size which appear in these tilings by two different method: one based on the substitutive structure of the Penrose tilings and the other on their definition by the cut and projection method. We use this to prove that the geometrical Penrose tilings are characterized by a small set of patterns called vertex-atlas, *i.e.*, they form a tiling space of finite type. Though considered as folk, no complete proof of this result has been published, to our knowledge.

1 Introduction

Penrose tilings are the tilings of the Euclidean plane by the fat and the thin rhombus with arrowed edges of Figure 1b. Two rhombi intersect in either a single vertex or a whole edge. In the latter case, the common edge of the two rhombi must be identically arrowed in each rhombus (orientation and single/double arrow).

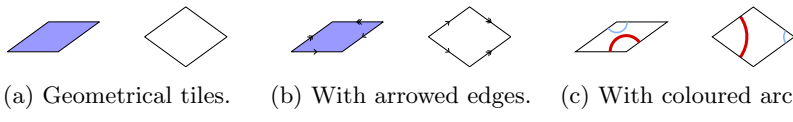


Figure 1: The Penrose rhombus tiles: all edges are of length 1, the thin rhombus has angles $\frac{\pi}{5}$ and $\frac{4\pi}{5}$, the fat rhombus has angles $\frac{2\pi}{5}$ and $\frac{3\pi}{5}$.

There are uncountably many different Penrose tilings, none of which being periodic. They all have the same finite patterns, that is, they are locally indistinguishable. Figure 2 shows such a tiling.

For better readability of the figures, we consider an alternate definition where arrows are replaced by coloured arcs (Fig. 1c) that must match on the edge of adjacent tiles, as in Figure 3. The type of the arrow is encoded by the colour of

*Université Aix-Marseille & Université de Caen

†Université Sorbonne Paris Nord, CNRS & HSE University

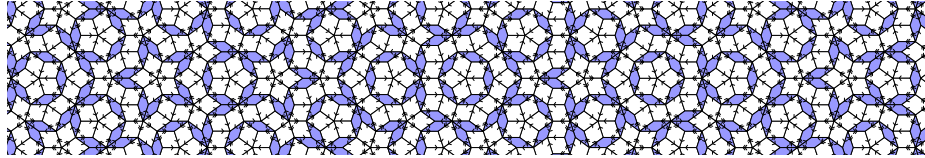


Figure 2: A Penrose tiling with arrowed rhombi.

the arc, and the orientation by the intersection point of the arc with the edge which is offset in one direction and not in the middle of the edge.

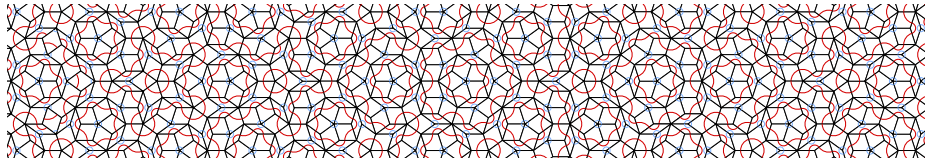


Figure 3: A Penrose tiling with coloured-arc rhombi.

If we remove the arrows or coloured arcs from the tiles of a Penrose tiling, we get a tiling by two types of rhombus (Fig. 4). We call these the *Geometrical Penrose tilings*. The question we are here interested in is: are the Geometrical Penrose tilings characterized by their patterns of a given finite size? In dynamical terms: does the *tiling space* formed by the Geometrical Penrose tilings (with removed arrows) have *finite type*?

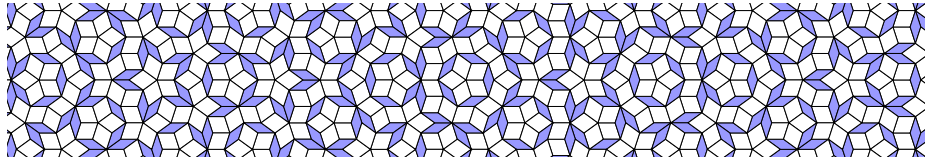


Figure 4: A Penrose tiling where arrows or coloured-arcs have been removed.

Definition 1 (k-map and k-atlas) *A k-map of a rhombus tiling is a pattern formed by all the tiles which have a vertex at edge-distance at most k from a given vertex. For example, the rhombi which share a vertex is a 0-map. The set of all the k-maps of a tiling (or tiling space) is called the k-atlas or k-vertex-atlas.*

Remark 1 *The vertices of a k-map centered in x are exactly the union of:*

- *the vertices within distance k from x;*
- *the vertices at distance k + 1 from x (they all belong to a tile which has a vertex at distance k);*

- the vertices at distance $k + 2$ from x that have two neighbors at distance $k + 1$ from x (they belong to a tile with one vertex at distance k from x , two at distance $k + 1$ and one at distance $k + 2$), see Fig.5.

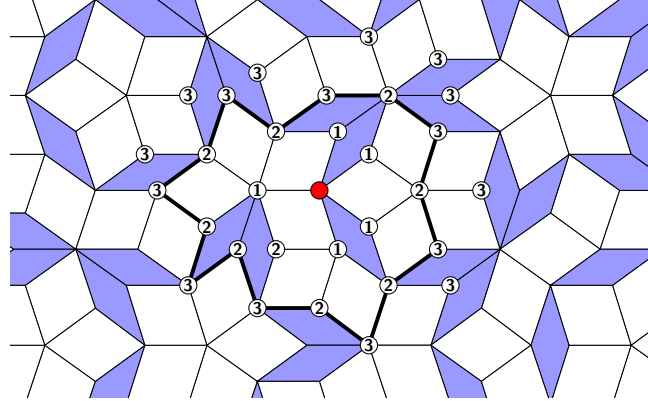


Figure 5: A 1-map centered on the red point, with its boundary emphasized. The numbers give the distance to the red point.

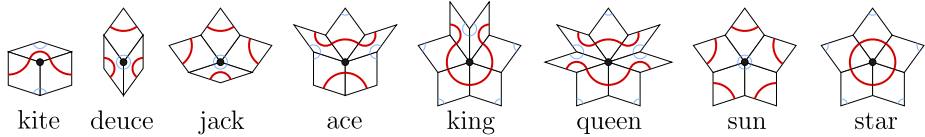


Figure 6: The 0-atlas of Penrose tilings with coloured arcs (up to isometry), the name of the 0-maps come from [4].

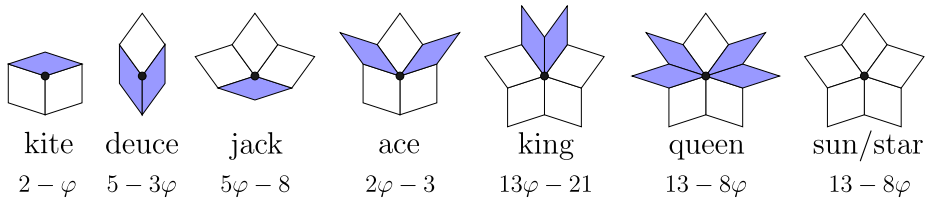


Figure 7: The 0-atlas of geometrical Penrose tilings (up to isometry), the numbers are the frequencies of the patterns with $\varphi = (1 + \sqrt{5})/2$ the golden ratio.

The 0-atlas of Penrose tilings is known [7] to contain exactly 8 0-maps with labels (Fig. 6) and 7 0-maps without labels (Fig. 7). Despite a common belief, the 0-atlas does not characterize geometrical Penrose tilings, that is, there exist tilings of the whole plane whose 0-maps all belongs to the 0-atlas of Penrose tilings but which are not Penrose tilings (Fig. 8).

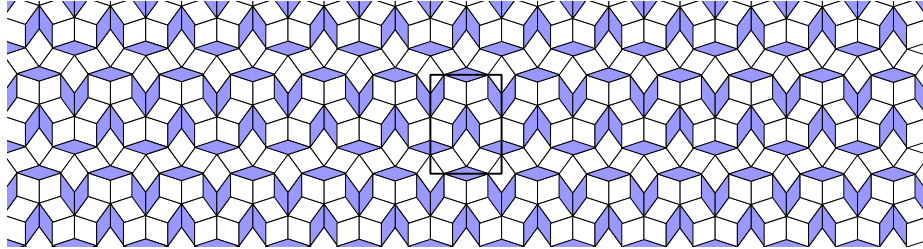


Figure 8: A periodic tiling whose 0-maps belong to the 0-atlas of Penrose tilings.

Here we show the following fact, which is often considered as folk:

Theorem 1 *Penrose tilings are characterized by their 1-atlas.*

A similar result appears in [7] (Theorem 6.1 p. 177):

Theorem 2 ([7]) *Any tiling of the plane by T and t rhombs whose **stars** are restricted to the 7 types shown in Fig. 7 is a Penrose tiling, provided that no two **stars** that share a rhombus are related by a half turn around the center of that rhomb.*

In this statement, T and t are the thick and thin Penrose rhombus tiles, and **stars** are the 0-maps (and not the star pattern of Figure 6).

The proof of this proposition in [7] mostly considers the case of the *sun/star* pattern, which is composed of 5 thick rhombi around a vertex and can be labelled in two ways, and suggests that it is the only difficult case. A simple evidence of the fact that the sun/star pattern is not the only problematic case is that the periodic tiling of Fig. 8 does not contain the sun/star pattern.

Rather than to complete the proof of the statement by Sénéchal, we rather reformulate it as Th. 1, which we hope is less likely to be misunderstood.

In Section 2 we present the 1-atlas of Penrose tilings and prove that the 1-atlas we present is correct. In Section 3 we prove that this 1-atlas indeed characterizes Penrose tilings.

2 Finding the 1-atlas of Penrose tilings

The first step to prove Theorem 1 is to find the 1-atlas of Penrose tilings.

Proposition 1 *The 1-atlas of Penrose tilings is exactly the 15 patterns up to isometry represented in Figure 9.*

This can be proved in many different ways. The natural idea would be to perform a combinatorial exploration of all the 1-maps with labelled tiles and then to remove the labels. However this might not be sufficient because there exist *deceptions*[2], *i.e.*, finite labelled patterns that satisfy the matching rules induced by the labels but that do not appear in any infinite

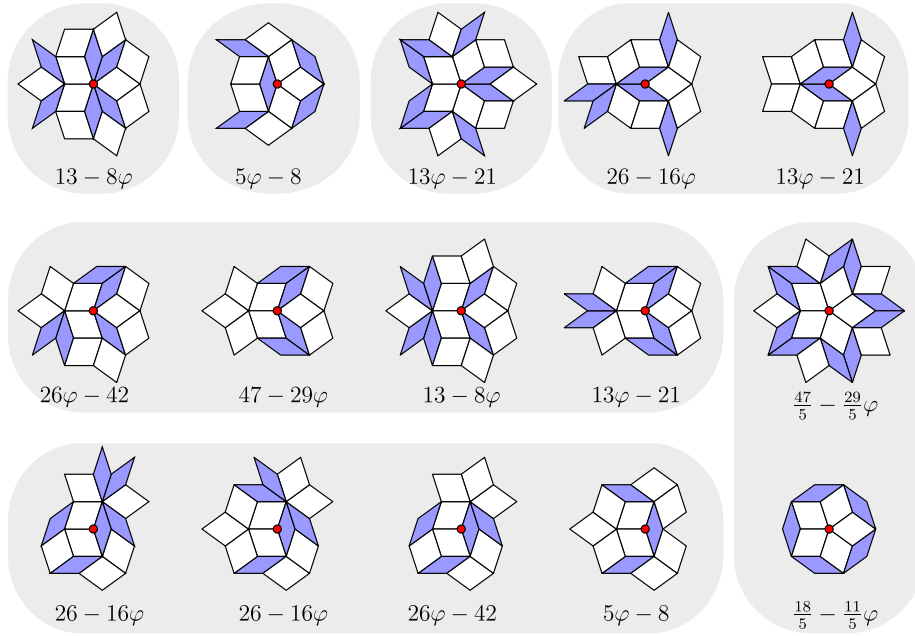


Figure 9: The 1-atlas of Penrose tilings (up to isometry, grouped by 0-maps), the numbers are the frequencies of the patterns with $\varphi = (1 + \sqrt{5})/2$ the golden ratio.

Penrose tiling (see Fig. 10). Some deceptions are easy to eliminate as such from the output of our combinatorial exploration, but some might be extremely hard to eliminate.

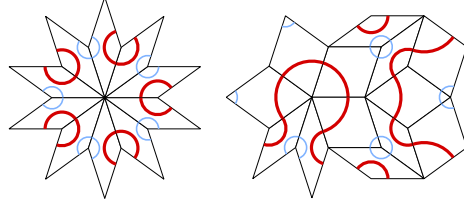


Figure 10: Two simple examples of *deceptions*: patterns that are allowed by the local rules but that cannot be extended to full tilings of the plane.

Rather than this combinatorial exploration, we present two methods, the first one uses the substitutive definition of Penrose tilings and the second one uses the cut-and-project definition of Penrose tilings. Note that the second methods also gives frequencies of appearance for each 1-map.

2.1 Finding the 1-atlas using substitutions

In this method we use the substitutive property of Penrose tilings, to obtain the linear recurrence of Penrose tilings with an explicit upper bound for the ratio of linear recurrence, hence we can obtain a finite region of the canonical Penrose tiling that contains all the 1-maps.

A *substitution* σ is an inflation-subdivision function that maps each tile to a set of tiles, see Fig. 11. It is called vertex-hierarchic when there exists a linear map called *expansion* φ such that for any tile t the vertices of $\varphi(t)$ are boundary vertices of the patch of tiles $\sigma(t)$, in Fig. 11 the expansion is drawn in dotted lines. Here we are interested in the case of the expansion being a direct similitude, we consider the expansion as the multiplication by a scalar and we write $\varphi(t)$ as $\varphi \cdot t$ where φ is the expansion factor.

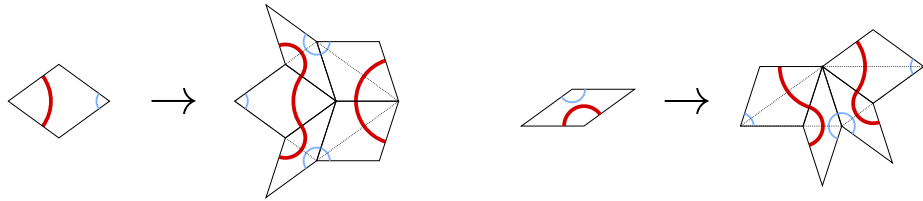


Figure 11: The Penrose substitution σ .

A substitution σ is called *primitive* when there exists an integer k such that for any tile t , the patch $\sigma^k(t)$ contains all the tiles in the tilesset (in every orientation).

A substitution σ defines the subshift (or set of tilings) X_σ of regular σ -tilings defined as the set of tilings \mathcal{T} such that any finite patch $P \in \mathcal{T}$ appears in some $\sigma^k(t)$ for $k \in \mathbb{N}$ and t a single tile.

Given a pattern P and a set of tilings X (or a single tiling \mathcal{T}), we call *appearance radius* of P the infimum of the radii r such that the pattern P appears in any disk of radius r in any tiling in X .

When the appearance radius of every pattern is finite, the tiling or set of tilings is called *uniformly recurrent* or *uniformly repetitive*. When, additionally, there exists a constant C such that for any pattern P the appearance radius of P is at most the radius of P multiplied by C , then the tiling or set of tilings is called *linearly recurrent* with recurrence factor C .

Lemma 1 ([8], Linear Recurrence) *Let \mathbf{T} be a tileset such that edge-to-edge tilings of tileset \mathbf{T} have finite local complexity. Let σ be a primitive vertex-hierarchic substitution with the expansion being a similitude of scaling factor $\varphi > 1$.*

Any σ -tiling is linearly recurrent with recurrence factor at most

$$C := \frac{\varphi C_0}{C_1}$$

where C_0 is the recurrence radius of the 0-maps in the σ -tiling and C_1 is a radius such that any disc of radius $r < C_1$ in a \mathbf{T} -tiling is entirely covered by a 0-map.

Remark 2 Note that primitive substitution tilings are uniformly recurrent, hence the existence of C_0 .

Note that in [8] this lemma is stated for self-similar tilings, i.e., regular tilings for an edge-hierarchic substitution (the union of the tiles in $\sigma(t)$ is exactly the expanded tile $\varphi(t)$) whose expansion is a similitude, but the important thing is that the substitution is an expansion-subdivision process with the expansion a similitude of scaling factor $\varphi > 1$.

Note also that the hypothesis of the expansion being a similitude is necessary, for example see the substitution of Appendix A.

Note also that for the 1-atlas we are interested in the appearance radius of the 1-maps up to isometry, so we are interested in the "up-to-isometry" recurrence factor.

Lemma 2 (Linear recurrence factor for Penrose tilings) *The Penrose rhombus tilings are linearly recurrent with a recurrence factor up to isometry at most C_p with*

$$C_p := \frac{\varphi \cdot (1 + \varphi + \sqrt{19 + 30\varphi})}{2 \cos(\frac{2\pi}{5}) \sin(\frac{2\pi}{5})} < 29.830.$$

Remark 3 Note that this statement and proof concern labelled (arrowed or with coloured arcs) Penrose rhombus tilings. They imply the same result for Geometrical Penrose rhombus tilings.

Note also that this bound is not optimal, however it is hard to find an optimal value because the asymptotic ratio of appearance radius by the radius of the pattern is 1 because Penrose tilings are densely repetitive [6]. So the bound is not asymptotic but is reached for some finite pattern (probably of relatively small size) and finding it would require a very extensive combinatorial exploration and then a computer assisted proof.

Proof. Let us first recall that Penrose tilings are substitution tilings with the substitution σ of Figure 11 which is vertex-hierarchic and has scaling factor $\varphi = \frac{1+\sqrt{5}}{2}$, note that φ is the golden ratio and that $\varphi^2 = \varphi + 1$.

In order to apply Lemma 1 we now compute C_0 and C_1 for Penrose tilings. C_1 is precisely the inner radius of the narrow rhombus tile,

$$C_1 = 2 \cos\left(\frac{2\pi}{5}\right) \sin\left(\frac{2\pi}{5}\right) \approx 0.588.$$

Indeed a circle of radius more than C_1 centered on the center of a narrow Penrose rhombus overlaps on all four sides of the tile and hence is not covered by a single 0-map. And a circle of radius at most C_1 is either completely covered by a tile, overlaps along two adjacent edges or overlaps along only one edge. In all three cases it is covered by a single 0-map.

C_0 is harder to compute. Recall that we are interested in the appearance radius of the 0-maps in the labelled Penrose rhombus tilings. There are 8 labelled 0-maps (Fig. 6).

We give and upper and lower bound $r_c \leq C_0 \leq r_c + r_v$ with $r_c := \sqrt{19 + 30\varphi}$ and $r_v := 1 + \varphi$. To prove this bound we again use the Penrose substitution : any Penrose tiling \mathcal{T} is the image of a Penrose tiling \mathcal{T}_{-1} by the substitution, which itself is also the image of a Penrose tiling by the substitution. Let us take a Penrose tiling \mathcal{T} , there exists a Penrose tiling \mathcal{T}_{-3} such that $\mathcal{T} = \sigma^3(\mathcal{T}_{-3})$. This induces a decomposition of \mathcal{T} in *metatile*s of order 3, *i.e.*, the image by σ^3 of the tiles in \mathcal{T}_{-3} (Fig. 12).

Let us denote r_v the maximal distance from a point of \mathbb{R}^2 to the closest corner of a metatile of order 3 and r'_v the maximal distance from a point of \mathbb{R}^2

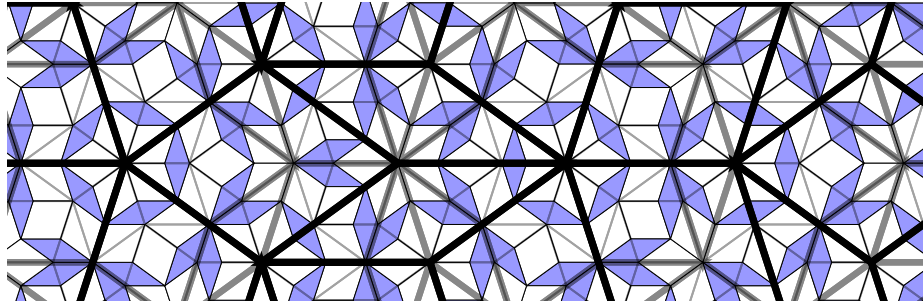


Figure 12: The decomposition of a geometrical Penrose tiling in metatile of order 1 (thin grey lines), 2 (bold grey lines) and 3 (bold black lines).

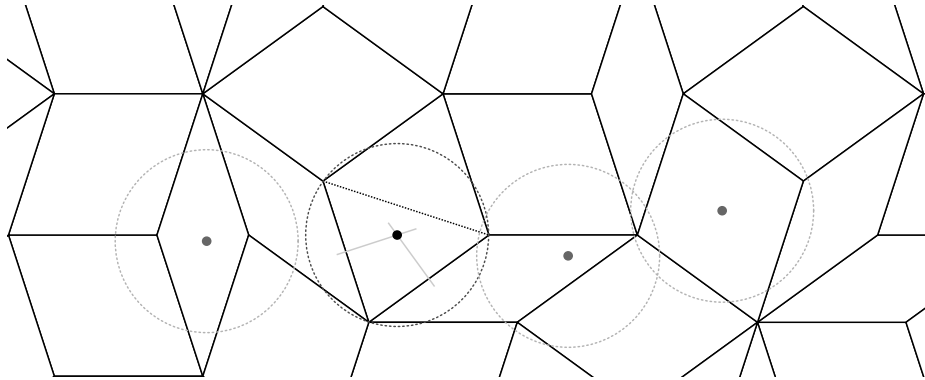


Figure 13: The maximal distance r'_v from a point of \mathbb{Z}^2 to a vertex of a Penrose tiling is the radius of the circle circumscribed to the half fat rhombus.

to the closest vertex in a Penrose tiling. We have $r_v = \varphi^3 r'_v$. We also have that r'_v is exactly the radius of the circumscribed circle to the triangle consisting of the thick Penrose rhombus bisected along its short diagonal (Fig. 13), so we have

$$r_v = \varphi^3 r'_v = \frac{\varphi^3}{2 \sin(3\pi/10)} = \varphi^2 = 1 + \varphi.$$

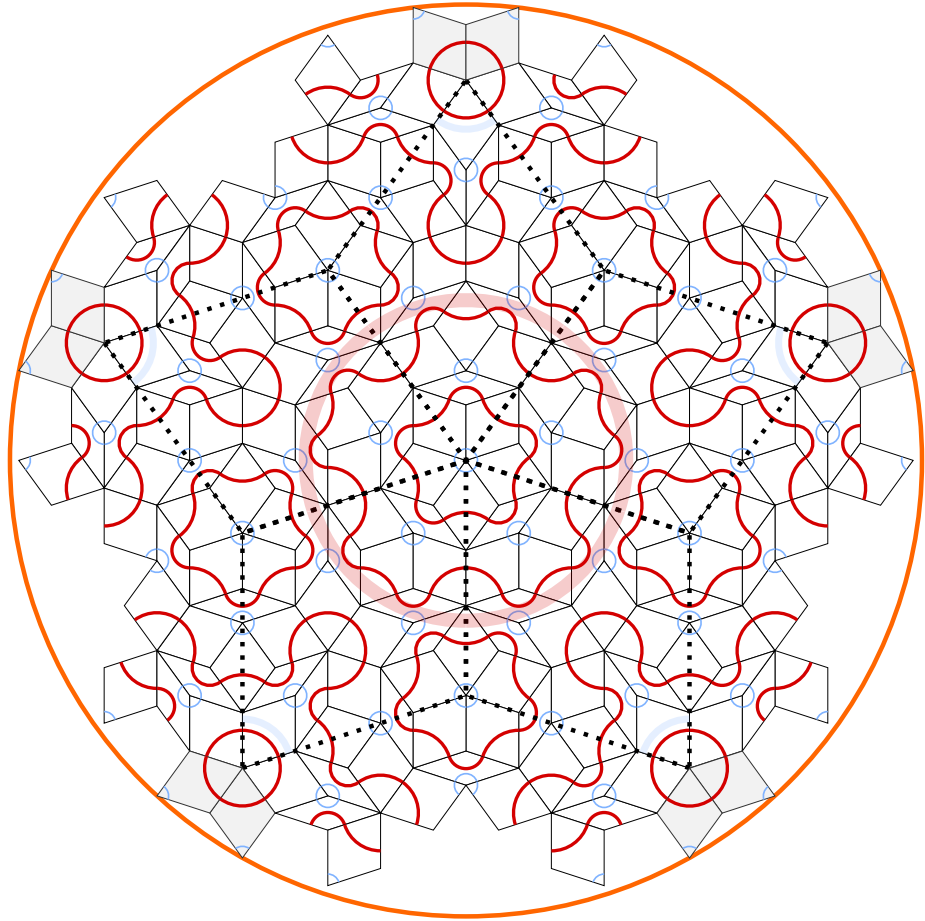


Figure 14: The third image by σ of star pattern, all the 0-maps appear in the circle of radius r_c the bound is reached for the star pattern. Note that in these star patterns, only 3 tiles are actually in the image $\sigma^3(star)$ but the remaining 2 tiles are forced by the fact that the center of this pattern is also a center of $\sigma^3(deuce)$ (because each star pattern is surrounded by deuce patterns) which has a star at its center.

We now denote r_c the appearance radius of the 0-maps up to isometry around the center of third order metatiles 0-maps, *i.e.*, the image of 0-maps by σ^3 , see Fig. 15. We have $r_c = \sqrt{a^2 + b^2 - abc}$ with

$$a := 3(1 + \varphi) \quad b := 1 \quad c = 2 \cos \frac{3\pi}{5} = 1 - \varphi,$$

we simplify with $\varphi^2 = \varphi + 1$ and we obtain $rc = \sqrt{19 + 30\varphi}$. This bound is reached by the appearance of radius of the sun around the center of third image of the sun, see Fig. 14 and 15.

We obtain the expected bounds $r_c \leq C_0 \leq r_c + r_v$, indeed the appearance radius of the 0-maps around a point of \mathbb{R}^2 is at most the distance from this point to a corner of third order metatile plus the appearance radius around this corner of third order metatile.

Now we apply Lemma 1 to obtain the expected bound $\varphi C_0 / C_1 \leq \varphi(r_c + r_v) / C_1$. \square

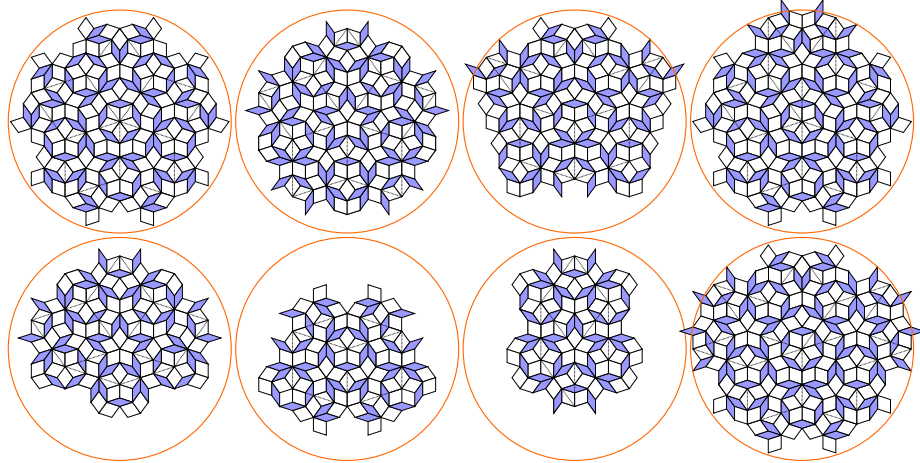


Figure 15: The third image by σ of the geometrical Penrose 0-maps, in each patch there is a copy of each 0-maps up to isometry that lies inside the circle of radius r_c , recall that the sun/star pattern must appear in both sun and star orientation.

Remark that the radius of the 1-maps is bounded by $1 + 2 \cos(\pi/10)$. Which means that, by linear recurrence, all the 1-maps must appear up to isometry in any patch of radius $R_{A_1} = (1 + 2 \cos(\pi/10))C < 86.57$.

In particular this holds for the central disc of radius R_{A_1} in the canonical Penrose Tiling. Since the canonical Penrose Tiling has global 5-fold symmetry and a reflexion symmetry around the horizontal axis we can reduce the disc to a $\pi/5$ cone of the disc.

We define P_{A_1} the patch of the canonical Penrose tiling of tiles that are in the central disc of radius R_{A_1} and are at edge distance at most 1 of the cone of angle

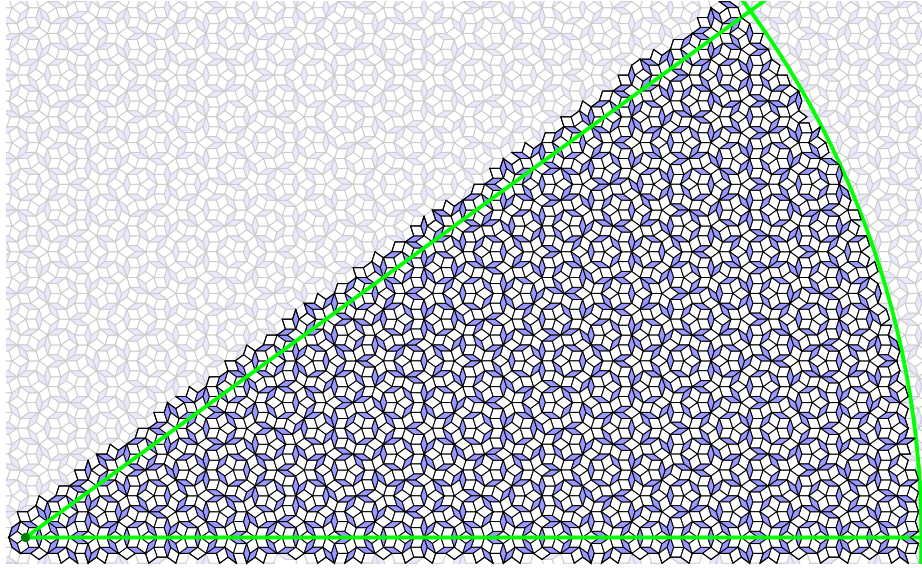


Figure 16: The patch P_{A_1} in which all the 1-maps of the Geometrical Penrose tiling appear, in green the cone of angle $\pi/5$ and the circle of radius 86.57.

$\pi/5$, see Fig. 16. The 1-atlas up to isometry appears in P_{A_1} . We enumerate all the 1-maps in this finite pattern and we obtain the 1-atlas presented in Figure 9.

Remark 4 *Another proof using the substitution would be to build the directed graph of 1-maps under the substitution, i.e., a directed graph $G = (V, E)$ such that the vertices $v \in V$ are 1-maps and there is an edge $u \rightarrow v$ if the 1-map v appears in $\sigma(u)$ up to isometry. To build this graph we can start from a single 1-map, for example the extended sun, and iterate the substitution until no new vertices are added, see Appendix C.*

2.2 Finding the 1-atlas using cut-and-projection

This method uses the cut-and-project property of Penrose tilings as explained in [3], using the notions of *window* and *region* of a pattern.

Definition 2 *Let E be a d -dimensional affine plane in \mathbb{R}^n which does not contain any rational line and such that the boundary of $E + [0, 1]^n$ does not intersect \mathbb{Z}^n . Let π denotes the orthogonal projection onto E . The cut and project tiling with slope E is defined as follows:*

1. select (cut) the d -dim. unit facets of \mathbb{Z}^n which lie inside $E + [0, 1]^n$;
2. project them under π to get a tiling of E .

For example, the cut and project tilings whose slope is a 2-plane of \mathbb{R}^5 directed by the two vectors

$$(\cos \frac{2k\pi}{5})_{0 \leq k \leq 5} \quad \text{and} \quad (\sin \frac{2k\pi}{5})_{0 \leq k \leq 5}$$

are called *generalized Penrose tilings*. Among them, the Penrose tilings correspond to affine slopes which contain a point whose coordinate sum up to an integer.

The fact that the cut and project method indeed defines a tiling is proven in [1]. The selected facets actually form a d -dim. surface and the projection π is a homeomorphism between this surface and E . The *lift* of a vertex x of the tiling, denoted by \hat{x} , is the unique point of this surface which projects onto x .

Definition 3 Let π' denote the orthogonal projection onto the orthogonal complement E' of E . The *window* of a cut and project tiling with slope E is the $(n-d)$ -dimensional polytope

$$W := \pi'(E + [0, 1]^n).$$

For $x' \in W$ and $k \in \mathbb{N}$, define the set $B(x', k)$ of points u of \mathbb{Z}^n of 1-norm at most k and such that $x' + \pi'u$ is still in the window W , i.e.,

$$B(x', k) := \{u \in \mathbb{Z}^n, \|u\|_1 \leq k, x' + \pi'u \in W\}$$

and denote by $V(x', k)$ the vertices in $B(x', k+2)$ which have at least two neighbors in $B(x', k+1)$, where u and v are neighbors if $\|u-v\|_1 = 1$. Hence, if there is a vertex x of the tiling such that $\pi'\hat{x} = x'$, then $x + \pi V(x', k)$ is exactly the set of vertices of the k -map centered on x (recall Remark 1). This definition however holds for any $x' \in W$, not only for the countably many which are in $\pi'\mathbb{Z}^n$. Now, define

$$R(x', k) := \bigcap_{u \in V(x', k)} (W - \pi'u).$$

This is a polytope included in W , called a *k-region* of the tiling.

Proposition 2 The image by π' of an integer point \hat{y} in $E + [0, 1]^n$ is in $R(x', k)$ iff its image by π is the center of a k -map with vertices $\pi\hat{y} + \pi V(x', r)$.

Proof. The only difficulty is in the formalism:

$$\begin{aligned} \pi'\hat{y} \in R(x', k) &\Leftrightarrow \forall u \in V(x', k), \pi'\hat{y} \in (W - \pi'u) \\ &\Leftrightarrow \pi'(\hat{y} + V(x', k)) \subset W \\ &\Leftrightarrow \hat{y} + V(x', k) \subset E + [0, 1]^n \\ &\Leftrightarrow \pi\hat{y} + \pi V(x', r) \text{ are vertices of the tiling.} \end{aligned}$$

The definition of $V(x', r)$ yields that those are the vertices of a k -map. \square

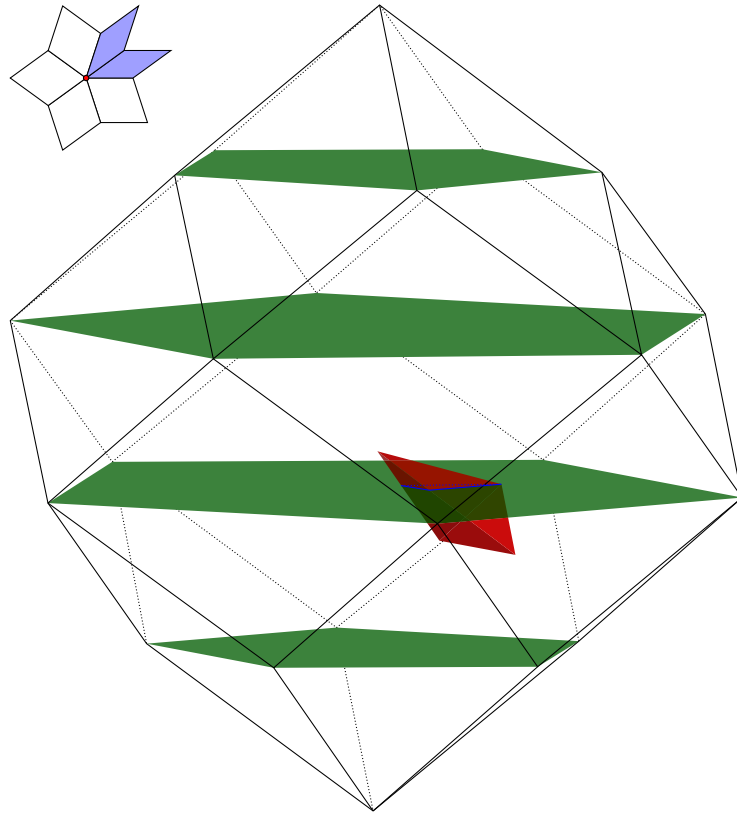


Figure 17: The window of a Penrose tiling is a rhombic icosahedron. Top-left, a 1-map is depicted. The corresponding region is the red tetrahedron in the window. The slope of generalized Penrose tilings is however specific: it is contained in a four dimensional rational subspace of \mathbb{R}^5 (namely the space orthogonal to $(1, 1, 1, 1, 1)$) and the points of $\pi' \mathbb{Z}^5$ are not dense in the window but form a family of parallel planes (whose intersection with the window is here depicted in green). Hence, only the regions which intersect these planes will indeed correspond to patterns, as it is the case here with the red tetrahedron. Shifting the slope shifts these planes which may intersect different regions: this means that two generalized Penrose tilings may have different finite patterns. Recall that Penrose tilings have been defined as generalized Penrose tilings with a slope which contains a point whose coordinates sum up to 1. This amounts to fix the green parallel planes to go through the vertices of the window, hence to always intersect the same regions. This is why Penrose tilings have all the same finite patterns.

In other words, there is an explicit bijection between the k -maps of the tiling (considered up to translation) and its k -regions. More exactly, we have to consider only the k -regions which contain the image by π' of an integer point, which is generic (since $\pi'\mathbb{Z}^n$ is generically dense in E'). However, Penrose's case is precisely not generic, as explained in Fig. 17.

Now, the point is that, for every $x' \in W$, both $V(x', k)$ and $R(x', r)$ can be easily computed (it amounts to checking that projections of whole points are in a polytope or intersecting whole translates of polytopes). And this is done in an exact way with computer algebra if E as well is given in an exact way (for example if it is generated by algebraic vectors). This leads to Algorithm 1 to compute the k -atlas of a tiling.

Algorithm 1: Computing a k -atlas

Data: d -dim. affine plane E in \mathbb{R}^n , integer k

Result: the list of the k -maps of the cut and project tiling with slope E

```

 $A \leftarrow [];$ 
 $R \leftarrow \emptyset;$ 
 $x' \leftarrow$  random point in  $W$ ;
while  $R \neq W$  do
  append  $V(x', k)$  to  $A$ ;
   $R \leftarrow R \cup R(x', r)$ ;
   $x' \leftarrow$  random point in  $W \setminus R$ ;
return  $A$ ;
```

Applying this algorithm with the slope E of generalized Penrose tilings yields a 0-atlas of 153 patterns and a 1-atlas of 1705 patterns. Up to isometry, these sets respectively reduce to 16 and 110 patterns. These are all the patterns which appear in the generalized Penrose tilings. To obtain the 0-atlas with 7 patterns depicted in Fig. 7 or the 1-atlas with 15 patterns depicted in Fig. 9, which are the patterns which appear in Penrose tilings only, we need to take into account that the slope E of Penrose tilings is such that the points of $\pi'\mathbb{Z}^n$ are not dense in W but lies in parallel planes: only the regions intersected by these planes indeed correspond to pattern of the tilings (Fig. 17, see also Remark 6).

Remark 5 Let us mention that a similar approach is used in [5] to compute the complexity of cut and project tilings, but their regions may be not polytopal and even not connected. This is because they do not consider k -maps but vertices within Euclidean distance k from a given center. This is illustrated in Fig. 18.

Remark 6 We mention that the points of $\pi'\mathbb{Z}^n$ are generically dense in W . Actually, they are even uniformly distributed, that is, the proportions of integer points of norm at most k which project by π' inside some region in W tends, when n goes to infinity, to the ratio between the volume of this region and the volume of the window. In other words, computing these volume ratio yields the frequencies of each k -map. This is how the frequencies of 0-maps and 1-maps of

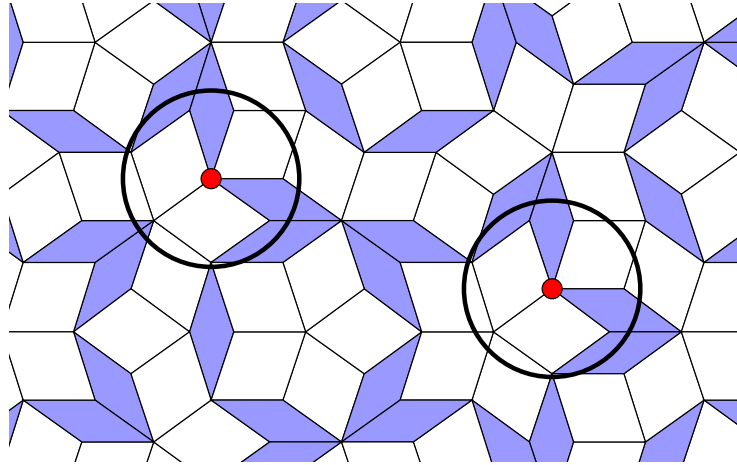


Figure 18: The 0-maps P_0 centered around the two red vertices are identical. However, the 1-maps P_1 and P_1' centered around the two red vertices are different (two thin blue tiles in the left one correspond to one large white tile in the right one). The regions of P_1 and P_1' are thus disjoint and may actually be not even adjacent (though they are subset of the region of P_0). Now, consider the sets of vertices inside these two circles. They are identical. Hence they correspond to the same region in the sense of [5]. But these vertex sets can be extended either as P_1 or as P_1' , their common region must contain a subset of both the regions of P_1 and P_1' . The region of this vertex set may thus be not connected.

the Penrose tilings (given in Fig. 9) have been computed, with the particularity that in the Penrose case, the points $\pi'\mathbb{Z}^5$ are uniformly distributed not in the whole window W but in parallel planes, so it is necessary to calculate the ratio of the total area of the intersection of a region with the planes and the total area of the intersection of these planes with W .

3 \mathbf{A}_1 characterizes Penrose tilings

We now prove the second part of Theorem 1 which we formulate as the following lemma.

Lemma 3 *A tiling by the thin and fat rhombus tiles whose 1-atlas is a subset of the atlas \mathbf{A}_1 depicted in Figure 9 admits a valid Penrose labelling and therefore is a geometrical Penrose rhombus tiling.*

Proof.

Let \mathcal{T} be a tiling by the thin and fat rhombus tiles (without labels) whose 1-maps belong to the 1-atlas \mathbf{A}_1 of Fig. 9, we add labels to the tiles around each vertex as depicted in Figures 19 and 20.

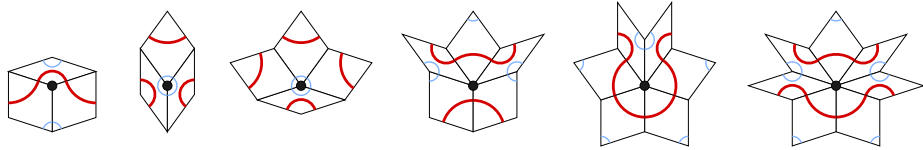


Figure 19: How to decorate the 6 first 0-maps. See Fig. 20 for the last case.

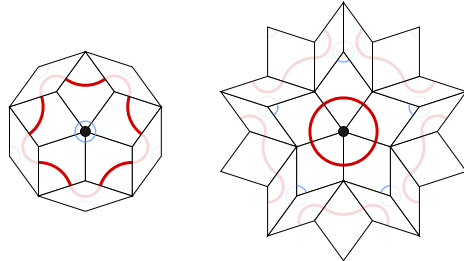


Figure 20: When a vertex is the center of a sun/star pattern, the 1-atlas shows that this 0-map can be extended in only two ways. This yields, once decorating tiles around the neighbour vertices as specified in Fig. 19, two possible decorations for this 0-map.

The label on any edge (arrows or coloured arcs) is thus defined by its endpoints. The only problem that may occur is that these endpoints yield different arrows! To show that this does not happen, we consider the *edge atlas* of Penrose tilings, that is, the set of patterns formed by the tiles which contain a vertex of a given edge. Since each pattern in the edge atlas is included in a 1-map, the edge atlas can be directly derived from Fig. 9. Otherwise it can also be directly computed through the methods used to prove Prop. 1.

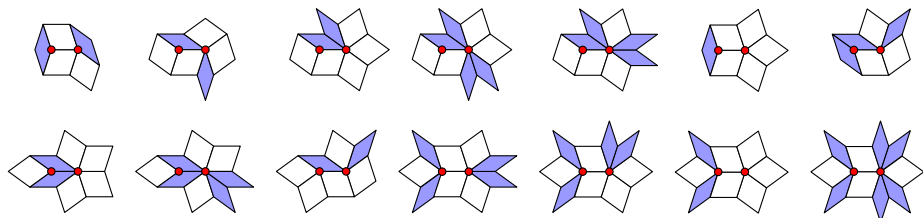


Figure 21: The edge atlas of Penrose tilings (up to isometry).

We can now check that the way arrows have been added on tiles around a vertex (Figures 19 and 20) is consistent for any two neighbour vertices. Recall that for the specific case of sun/star pattern, the labelling is consistent across the pattern and this can be seen either by looking at the edge-atlas patterns around the boundary of the sun/star or by the 1-atlas which allows only the sun and the star labellings which are both consistent across the pattern.

Hence, we get a tiling with rhombi labelled as the rhombi of Penrose tilings. By definition, this is a Penrose tiling. Hence the original unlabelled tiling is a geometrical Penrose tiling. Lemma 3 is thus proven.

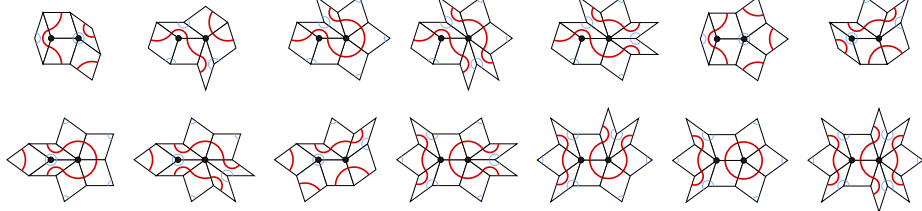


Figure 22: Consistence of the decorations around two connected vertices.

□

Combining Proposition 1 and Lemma 3 we obtain Theorem 1.

Remark that the edge-atlas of Fig. 21 also characterizes the geometrical Penrose tilings. Indeed the same proof holds for the first 6 0-maps, and for the case of sun/star by forcing the to have patterns of the edge-atlas around the boundary of a sun/star pattern we obtain only the two cases of the 1-atlas which correspond respectively to sun and to a star pattern. However we prefer the statement with the 1-vertex-atlas.

A A substitution whose tilings are not linearly recurrent

Here we present an example of substitution whose expansion is not a similitude (so Lemma 1 does not apply) and whose tilings are not linearly recurrent, in essence this example proves the fact that the hypothesis of the expansion being a similitude is necessary.

The substitution σ of Figure 23 on square tiles with labels 0 (or *white*) and 1 (or *black*) due to Solomyak (private communication) is primitive and yields uniformly recurrent tilings that are not linearly recurrent. Let τ be the Thue-Morse substitution $\tau : 0 \mapsto 01, 1 \mapsto 10$, the substitution σ is essentially τ with 0-padding above and below.

Recall a known fact on the Thue-Morse substitution : for any $n \geq 0$, the word $\tau^{n+1}(0)$ does not appear as a factor subword in $(\tau^n(0))^\omega$ (the periodic repetition of $\tau^n(0)$).

Let n be a positive integer. The rectangle pattern $\sigma^n(0^{3^n})$:

- is legal, indeed for any k the pattern 0^k is legal because it appears in the topmost line of $\sigma^{\lceil \log_2(k) \rceil}(0)$ so for any n , $\sigma^n(0^k)$ is legal because it appears in $\sigma^{n+\lceil \log_2(k) \rceil}(0)$ and in particular it holds for $k = 3^n$,

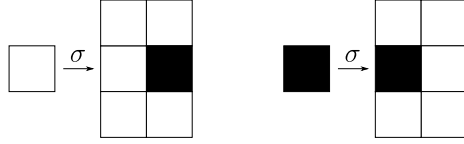


Figure 23: The substitution σ on square tiles with labels 0 (or *white*) and 1 (or *black*). Note that if we look only at the horizontal line we obtain the Thue Morse substitution, more precisely the substitution σ is just the Thue-Morse substitution τ with 0-padding above and below.

- has size $6^n \times 3^n$ indeed $\sigma^n(0^{3^n}) = (\sigma^n(0))^{3^n}$ and each $\sigma^n(0)$ has size $2^n \times 3^n$. In particular $\sigma^n(0^{3^n})$ has size more than $3^n \times 3^n$,
- does not contain the word $\tau^{n+1}(0)$ which is of size $2^{n+1} \times 1$ and which appears in $\sigma^{n+1}(0)$.

Let \mathcal{T} be a σ -tiling, by definition \mathcal{T} contains $\sigma^n(0)$ for any n . In particular, for any n it contains $\sigma^n(0^{3^n})$ and $\tau^{n+1}(0)$. So for any n , there exists a pattern of diameter 2^{n+1} that appears in the tiling, but does not appear in regions of size $3^n \times 3^n$, this is a contradiction to linear recurrence.

B Additional figures for the linear recurrence

Here we present 3 more figures regarding the patch $P_{\mathbf{A}_1}$ of the canonical Penrose tiling in which all 1-maps appear. In Figure 24 we have highlighted one occurrence of each 1-map up to isometry, in Figure 25 we have highlighted the occurrence closest to the center of each 1-map up to isometry, and in Figure 26 we present a minimal subpatch of $P_{\mathbf{A}_1}$ that contains one occurrence of all 1-maps up to isometry.

Remark that the appearance radius of the 1-maps seems to be much smaller than what we were able to prove.

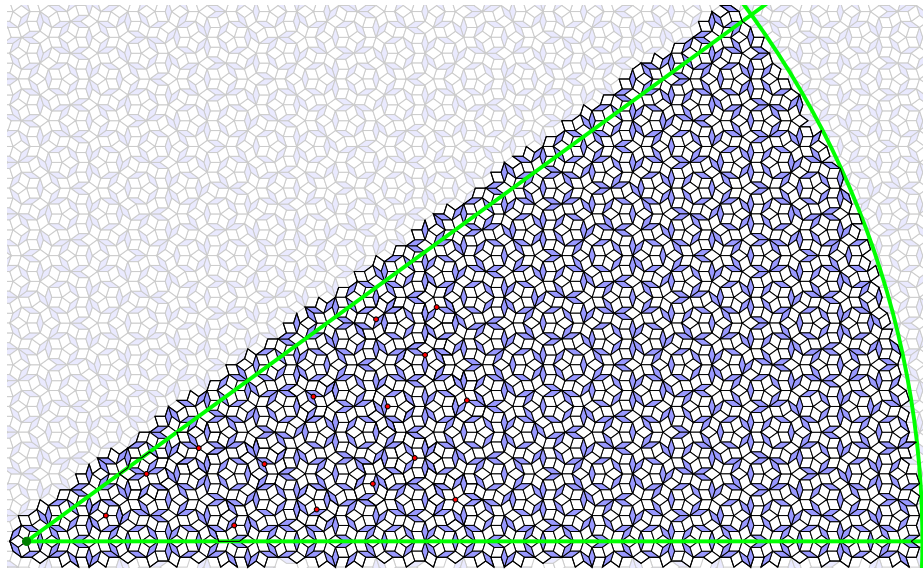


Figure 24: The patch P_{A_1} with scattered occurrences of the 1-maps highlighted.

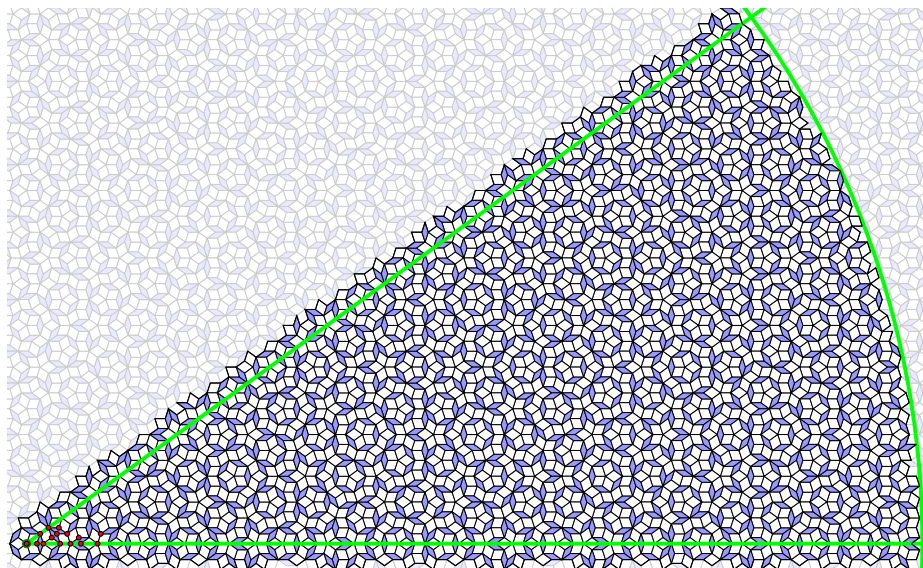


Figure 25: The patch P_{A_1} where the centers of the occurrence of each 1-map closest to the origin has been highlighted, we see that the 1-maps appear much closer to the origin than what our proof gives.

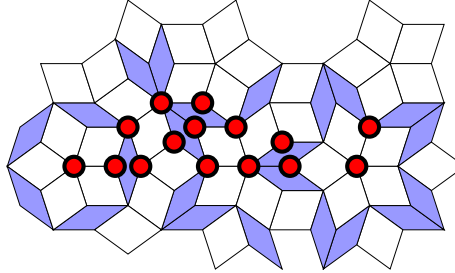


Figure 26: A minimal subpatch of $P_{\mathbf{A}_1}$ containing all the 15 1-maps, the center of the 1-maps are highlighted.

C 1-maps, substitution and graph

Another way to prove that the 1-atlas \mathbf{A}_1 presented in Fig. 9 is correct is to build the directed graph $G = (V, E)$ where V is the set of 1-maps and $u \rightarrow v \in E$ when v appears in $\sigma(u)$.

Since the Penrose substitution is primitive, we can start from a single pattern, for example take the 1-map that is the sun pattern surrounded by a layer of narrow rhombi, apply the substitution to obtain new vertices/1-maps and repeat until no new 1-map is generated, see Algorithm 2.

Algorithm 2: Computing the k -atlas with a primitive substitution σ and the corresponding graph.

Data: a well-defined primitive substitution σ and a k -map P_0
Result: the list of the k -maps of the σ -tilings up to translation

```

 $S \leftarrow [P_0];$ 
 $V \leftarrow [P_0];$ 
 $E \leftarrow [];$ 
while  $S \neq \emptyset$  do
   $P \leftarrow$  extract an element from  $S$ ;
  for  $P' \in \text{1maps}(\sigma(P))$  do
    if  $P' \notin V$  then
      append  $P'$  to  $V$ ;
      append  $P'$  to  $S$ ;
    append the directed edge  $(P, P')$  to  $E$ ;
return  $V$ ;
```

When we apply this algorithm (with the up-to-isometry equivalence on 1-maps) we obtain the graph depicted in Fig. 27, and the adjacency matrix of Fig. 28. In particular we obtain as expected the 1-atlas \mathbf{A}_1 .

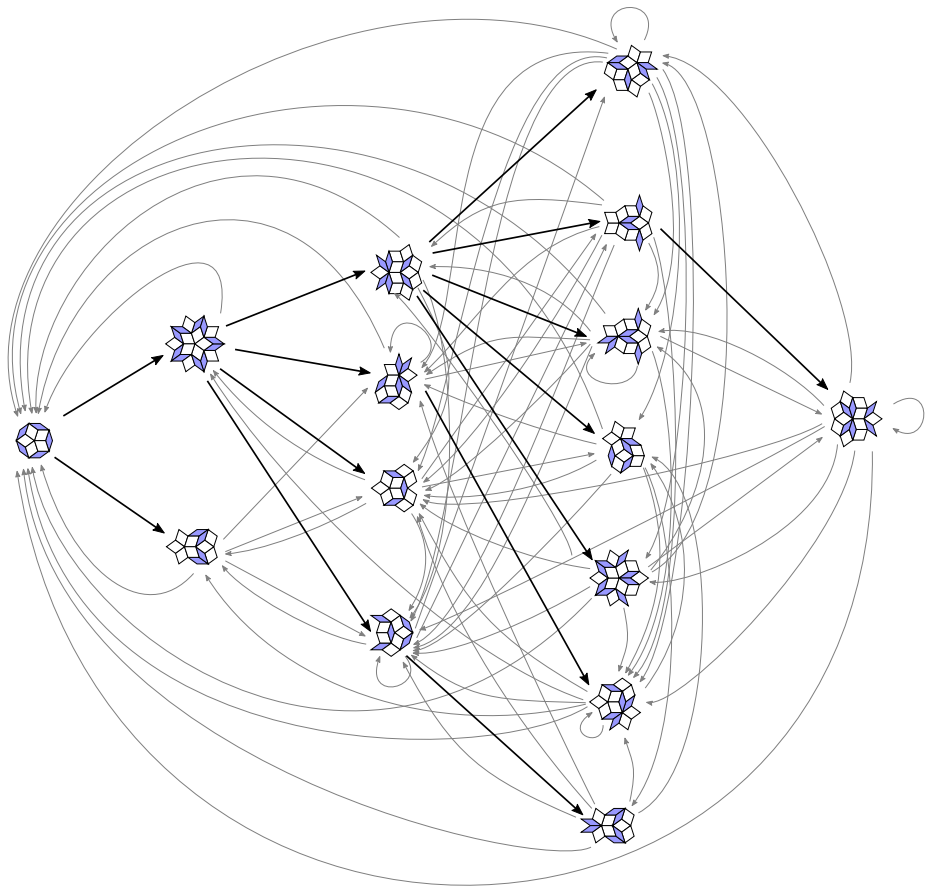


Figure 27: The graph $G = (V, E)$ of the 1-maps of Penrose tilings under the Penrose substitution σ , starting Algorithm 2 from the leftmost pattern, a bold black arrow indicates a new 1-map and grey arrows indicate a 1-map that was already explored.

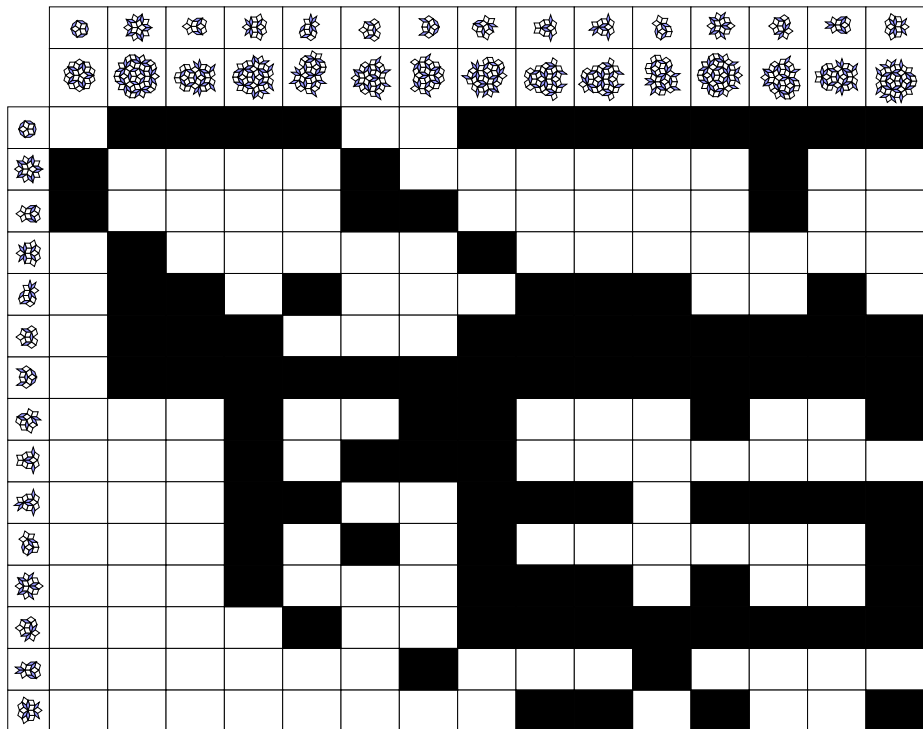


Figure 28: An "adjacency matrix"-like representation of the graph $G = (V, E)$ of the 1-maps of Penrose tilings under the Penrose substitution σ , the second line of column header are the images of the 1-maps by σ .

References

- [1] De Bruijn, N.G., *Dualization of multigrids*, J. Phys. Colloques, 1986.
- [2] S. Dworkin and J. I. Shieh, *Deceptions in quasicrystal growth*, Communications in mathematical physics, 1995.
- [3] Th. Fernique and C. Porrier, *A General approach to Ammann bars for aperiodic tilings*, LATIN 2022: Theoretical Informatics, 2022.
- [4] B. Grünbaum and G. C. Shephard, *Tilings and patterns*, Dover Publications, 1987.
- [5] H. Koivusalo and J. Walton, *Cut and project sets with polytopal window I: Complexity*, Ergodic Theory and Dynamical Systems, 2021.
- [6] D. Lenz, *Aperiodic linearly repetitive Delone sets are densely repetitive*, arXiv:math/0208132, 2002.
- [7] M. Senechal, *Quasicrystals and geometry*, Cambridge University Press, 1995.
- [8] B. Solomyak, *Nonperiodicity implies unique composition for self-similar translationally finite Tilings*, Discrete & Computational Geometry, 1998.